Letter

Pressure-induced transition from $J_{\text{eff}} = 1/2$ to $S = 1/2$ states in $CuAl_2O_4$

Hwanbeom Cho,[1,2,3,*] Choong H. Kim,[2,3] Yongmoon Lee,[4] Kazuki Komatsu,[5] Byeong-Gwan Cho,[6] Deok-Yong Cho,[7] Taehun Kim,[2,3,8] Chaebin Kim,[2,3,8] Younghak Kim,[6] Tae Yeong Koo,[6] Yukio Noda,[9] Hiroyuki Kagi,[5] Daniel I. Khomskii,[10] Donghoon Seoung,[11,†] and Je-Geun Park[2,3,8,12,‡]

[1]*Clarendon Laboratory, University of Oxford, Parks Road, Oxford OX1 3PU, United Kingdom*
[2]*Center for Correlated Electron Systems, Institute for Basic Science (IBS), Seoul 08826, Republic of Korea*
[3]*Department of Physics and Astronomy, Seoul National University, Seoul 08826, Republic of Korea*
[4]*Department of Geological Sciences, Pusan National University, Busan 46241, Republic of Korea*
[5]*Geochemical Research Center, Graduate School of Science, The University of Tokyo, Hongo, Bunkyo-ku, Tokyo, 113-0033, Japan*
[6]*Pohang Accelerator Laboratory, POSTECH, Pohang 37673, Republic of Korea*
[7]*IPIT & Department of Physics, Jeonbuk National University, Jeonju 54896, Republic of Korea*
[8]*Center for Quantum Materials, Seoul National University, Seoul 08826, Republic of Korea*
[9]*Institute of Multidisciplinary Research for Advanced Materials, Tohoku University, Sendai 980-8577, Japan*
[10]*II. Physikalisches Institut, Universität zu Köln, D-50937 Köln, Germany*
[11]*Department of Earth and Environmental Sciences, Chonnam National University, Gwangju 61186, Republic of Korea*
[12]*Institute of Applied Physics, Seoul National University, Seoul 08826, Republic of Korea*

(Received 21 December 2020; accepted 8 January 2021; published 3 February 2021)

The spin-orbit entangled (SOE) J_{eff} state has been a fertile ground to study quantum phenomena. Contrary to the conventional weakly correlated $J_{\text{eff}} = 1/2$ state of $4d$ and $5d$ transition metal compounds, the ground state of $CuAl_2O_4$ hosts a $J_{\text{eff}} = 1/2$ state with a strong correlation of Coulomb U. Here, we report that, surprisingly, Cu^{2+} ions of $CuAl_2O_4$ overcome the otherwise usually strong Jahn-Teller distortion and instead stabilize the SOE state, although the cuprate has relatively small spin-orbit coupling. From the x-ray absorption spectroscopy and high-pressure x-ray diffraction studies, we obtained definite evidence of the $J_{\text{eff}} = 1/2$ state with a cubic lattice at ambient pressure. We also found the pressure-induced structural transition to a compressed tetragonal lattice consisting of the spin-only $S = 1/2$ state for pressure $P_c > 8$ GPa. This phase transition from the Mott insulating $J_{\text{eff}} = 1/2$ to the $S = 1/2$ states is a unique phenomenon. Our study offers an example of the SOE J_{eff} state under strong electron correlation and its pressure-induced transition to the $S = 1/2$ state.

DOI: 10.1103/PhysRevB.103.L081101

Spin-orbit coupling (SOC) and a resulting quantum entangled state have been exciting research areas in condensed matter physics. Thanks to the extensive studies made over the past decade or so, it is now well known how SOC governs the physical properties of $5d$ transition metal oxides, particularly iridates [1–3]. Less well known is how this spin-orbit physics plays out under a strong electron correlation, i.e., at the regime of considerable Coulomb interaction. This question of strongly correlated spin-orbit physics seems to require two self-contradicting conditions. One is a sizeable SOC, which is inherently preferred for heavier elements like Ru and Ir [4]. The other is a strong electron correlation, which is favorable for lighter elements like $3d$ transition metals [5]. Hence, progress has been painfully slow in this quest despite much anticipation of rich and exotic physics.

When d orbitals are put under a cubic environment, the degenerate t_{2g} orbitals have the effective orbital angular momentum L_{eff}, leading to a spin-orbit entangled (SOE) J_{eff} state [1–3] with the entangled form of the spin and the orbital wave functions. Due to the partially quenched orbital angular momentum, the SOE state system has been an excellent playground to promote exotic quantum magnetism. In particular, the SOE $J_{\text{eff}} = 1/2$ state can lead to exchange anisotropy—a bond-dependent Ising type to host the Kitaev model [6–9]. A Mott insulating phase of the $J_{\text{eff}} = 1/2$ can be induced by a delicate balance among bandwidth W, Coulomb interaction U, and SOC λ [1,2]. As such, there have been reports of phase transitions induced by changing the balance via controlling the physical variables such as temperature and pressure in the systems with the SOE state [10–14].

Most studies on the SOE states have been so far focused on $4d$ and $5d$ transition metal compounds because the strong SOC ($\lambda = 100$–400 meV) [1,2,15,16] has been widely accepted as the most critical necessary condition to create such SOE states [17]. However, it is equally interesting to ask whether SOE states can be stabilized even in $3d$ transition metal compounds. Supposing they exist, they are anticipated to be quite different from those of the conventional J_{eff} states of $4d$ and $5d$ compounds with the relatively weak correlation ($U = 1.5$–2 eV) [1,2,15]. In that case, the J_{eff} states of $3d$ compounds will retain effects due to a strong correlation

*hwanbeom.cho@physics.ox.ac.uk
†dseoung@jnu.ac.kr
‡jgpark10@snu.ac.kr

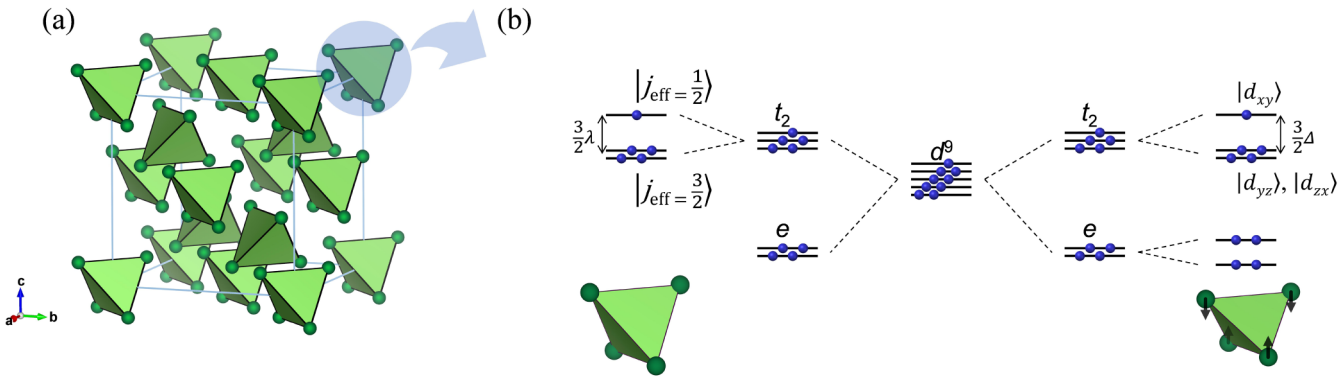

FIG. 1. (a) The unit cell structure of $CuAl_2O_4$. Cu^{2+} ions are located at the center of the tetrahedra made of four oxygen ions (green balls). The Al^{3+} ions are omitted for simplicity. The neighboring tetrahedra do not share a common oxygen ion and are separated from each other. (b) The ground state of $CuAl_2O_4$ at different regimes. (Left-hand side) If $\lambda > \Delta$, t_2 levels are split into the $j_{\rm eff} = 1/2$ and $j_{\rm eff} = 3/2$ states, and the CuO_4 tetrahedron retains its cubic symmetry. (Right-hand side) If $\lambda < \Delta$, t_2 levels are split into states with fully quenched orbital angular momentum, and the tetrahedron becomes tetragonally compressed along its local c axis.

($U > 5$ eV). Until now, this is a barely explored area of the phase diagram for different ratios of U and λ [1].

Our previous experimental [18,19] and theoretical papers [20,21] suggested a cuprate system $CuAl_2O_4$ (with Cu^{2+} in tetrahedra, having $e^4t_2^5$ electron configuration) as a strong candidate hosting the $J_{\rm eff} = 1/2$ state. As the Cu^{2+} ion has the largest U and λ among other magnetic $3d$ transition metals [4,5], the cuprate compound would be an excellent example to introduce the SOE state with a strong correlation. In this paper, using experimental techniques such as x-ray absorption spectroscopy (XAS) and high-pressure x-ray diffraction (XRD), we present the definite evidence of the $J_{\rm eff} = 1/2$ state in $CuAl_2O_4$ at ambient pressure and a structural transition to the state with $S = 1/2$ at high pressure.

$CuAl_2O_4$ has a spinel structure [Fig. 1(a)], where Cu^{2+} is located at the center of the tetrahedron (A site) [18,19]. Al^{3+} sits at the center of the octahedra that consists of six neighboring oxygen ions (B site). Due to the T_d point group symmetry of the crystal field, the $3d$ orbitals of Cu^{2+} ion in the tetrahedral site are split into upper t_2 and lower e orbitals. As depicted in the left-hand side of Fig. 1(b), one hole in the t_2 levels has $l_{\rm eff} = 1$. Note that capital $J_{\rm eff}$, $L_{\rm eff}$, and S ($j_{\rm eff}$, $l_{\rm eff}$, and s) stand for multiparticle (single particle) total, orbital, and spin angular momenta. The SOC further splits the t_2 levels into the SOE $j_{\rm eff} = 1/2$ doublet occupied by the single hole and the $j_{\rm eff} = 3/2$ states fully occupied by electrons. Finally, Coulomb interactions can give rise to a Mott insulating $J_{\rm eff} = 1/2$ state by splitting the $j_{\rm eff} = 1/2$ band.

However, on the other limit [right-hand side of Fig. 1(b)], where the energy scale of Jahn-Teller distortion $\Delta > \lambda$, an $S = 1/2$ state with fully quenched orbital angular momentum will be instead stabilized. At ambient pressure, our density functional theory (DFT) and dynamical mean-field theory calculations [20] predicted that, in $CuAl_2O_4$, the $J_{\rm eff} = 1/2$ state wins over the spin-only state. Although SOC is relatively small ($\lambda = 50$ meV) for Cu^{2+} ions, the strong correlation ($U = 7$ eV) works as if SOC is effectively enhanced to stabilize the $J_{\rm eff} = 1/2$ state. Since the $j_{\rm eff} = 1/2$ state occupied by the single hole involves the equal amount of t_2 orbitals ($\alpha' = 1/3$),

$$\left|j_{\rm eff} = \tfrac{1}{2}, j^z_{\rm eff} = \pm\tfrac{1}{2}\right\rangle = \sqrt{\alpha'}\left|l^z_{\rm eff} = 0\right\rangle|\pm\rangle - \sqrt{1-\alpha'}\left|l^z_{\rm eff} = \pm 1\right\rangle|\mp\rangle, \quad (1)$$

where $|l^z_{\rm eff} = 0\rangle = |d_{xy}\rangle$, $|l^z_{\rm eff} = \pm 1\rangle = -\frac{1}{\sqrt{2}}(i|d_{zx}\rangle \pm |d_{yz}\rangle)$, and $|\pm\rangle$ is the spin-half spinor [6], the CuO_4 tetrahedron is not distorted into D_{2d} symmetry but sustains instead the cubic (T_d) symmetry. The cubic symmetry of $CuAl_2O_4$ at ambient pressure was verified via low-temperature neutron diffraction [18] and XRD [19] methods. However, there is still a question of locally broken symmetry, which motivated this paper together with a possible pressure-induced new transition.

X-ray absorption near edge structure (XANES) measurement was done at the copper K edge to estimate the accurate value for site disorder in the single crystal. The other purpose was to confirm the lattice symmetry, i.e., the cubic structure without Jahn-Teller distortion. The observed spectrum in Fig. 2(a) has 10 peaks, which we can assign as peaks A to J. We can simulate the total spectrum by superposing two spectra, calculated with Cu^{2+} in the tetrahedral and octahedral sites of the cubic lattice, respectively, in the ratio of 64:36. The overall shape of the simulation consists of 10 peaks corresponding to the measurement, which indicates that the crystal indeed has the cubic lattice with the site disorder of $\eta = 0.36$, comparable with that obtained by the Rietveld method of the previous XRD data [19].

The tetrahedral site with T_d symmetry can form a p-d hybridized orbital, enabling the electric dipolar transition of $1s$ electron to the hybridized orbital [22,23]. The pre-edge peak A comes from a transition to the copper $3d$-$4p$ hybridized orbital in the tetrahedral site. In contrast, peak B originates from the hybridization of copper $4p$, oxygen $2p$, and aluminum $3s$ orbitals. On the other hand, the peaks C, D, F, H, J (E, G, I) arise from transitions to the copper p orbital states in the tetrahedral (octahedral) sites. This result is like the study on $CuAl_2O_4$ nanoparticles [24].

The intensity of the peaks in the experimental spectrum looks suppressed when compared with that in the calculation.

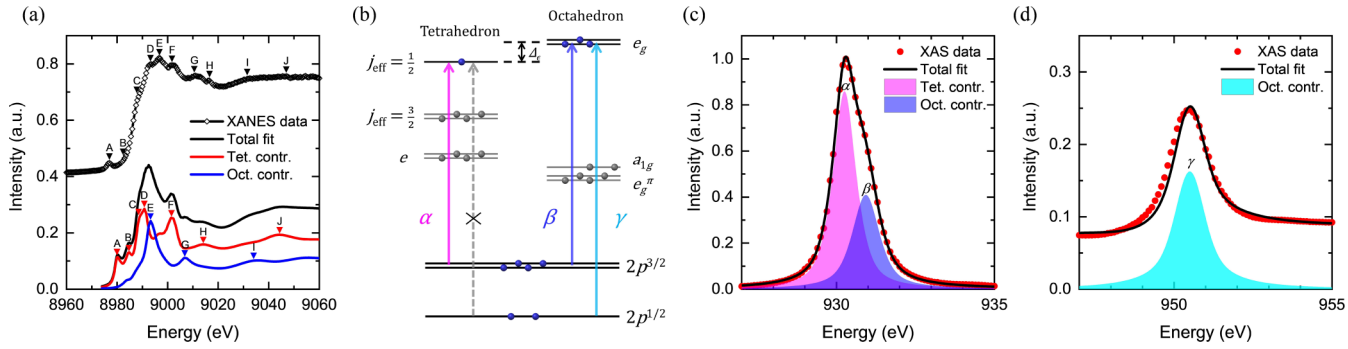

FIG. 2. (a) X-ray absorption near edge structure (XANES) spectrum at the copper K edge. The total spectral calculation done using the cubic lattice is composed of two contributions: 64 (36)% of Cu^{2+} ions located in the tetrahedral (octahedral) site. (b) Electric dipole transition occurring in the tetrahedral and octahedral sites. In the tetrahedral site, the transition at the L_3 edge (α) is allowed, but the transition at the L_2 edge is forbidden. However, in the octahedral site, the transitions at both L_3 and L_2 edges (β and γ, respectively) are allowed. (c) The observed absorption spectrum at the copper L_3 edge (∼930 eV). It has a distinct feature of two peaks: α and β. (d) The spectrum at the copper L_2 edge (∼950 eV). It features a single peak γ.

This is due to the self-absorption effect [25], which occurs when a single crystal is measured in a fluorescence yield mode. Moreover, since the simulation is based on a Hartree-Fock calculation with a muffin-tin potential [26], electron correlation is difficult to estimate precisely. This limitation can explain a difference in the position of the $3d$ band.

Copper L-edge XAS probes more directly the SOE character of the unoccupied state in $CuAl_2O_4$. This technique has so far been proven a useful tool to investigate the SOC of a ground state by using the electric dipole selection rules [15,27–29]. The $j_{\rm eff}=1/2$ state is branched off from the atomic $j=5/2$, $|j_{\rm eff}=1/2,\ j^z_{\rm eff}=\pm 1/2\rangle \propto \pm 1/\sqrt{6}\,|j=5/2,\ j_z=\pm 5/2\rangle \mp 5/\sqrt{30}|j=5/2,\ j_z=\mp 3/2\rangle$. If the hole in $CuAl_2O_4$ occupies the $j_{\rm eff}=1/2$ state, the transition from the $2p_{1/2}$ to $j_{\rm eff}=1/2$ states (L_2 edge) is forbidden, while the transition from the $2p_{3/2}$ to $j_{\rm eff}=1/2$ states (L_3 edge) is allowed. On the other hand, the transitions at both edges are allowed for the hole occupying a spin-1/2 state with fully quenched orbital angular momentum. Therefore, if the ground state of $CuAl_2O_4$ is indeed $J_{\rm eff}=1/2$, we expect to observe a single peak at the L_3 edge and no peak at the L_2 edge in the absorption spectrum.

However, there is a sizable amount of site disorder in our single-crystal sample: 64 (36)% of Cu^{2+} located in the tetrahedral (octahedral) site. Contrary to the octahedral site, where a hole occupies the e_g orbital state with $l_{\rm eff}=0$, the tetrahedral site can solely host the $j_{\rm eff}=1/2$ state. This will make an absorption peak α at the L_3 edge in the tetrahedral site, but the octahedral site will make two absorption peaks β and γ at the L_3 and L_2 edges, respectively [Fig. 2(b)]. Therefore, we expect to observe a three-peak feature, two peaks at the L_3 edge and a single peak at the L_2 edge, in the absorption spectrum.

From the XAS measurement of a single-crystal $CuAl_2O_4$, we verified that there are indeed two distinct peaks at the L_3 edge [Fig. 2(c)] and a single peak at the L_2 edge [Fig. 2(d)], as expected. At the L_3 edge, the ratio of the spectral weight of peaks α and β is estimated to be 0.636:0.364 [30], which is comparable with the above result of $\eta=0.36$ obtained from the XANES experiment. The spacing between the two peaks, 0.6(1) eV corresponds well to the energy difference $\Delta_\epsilon=0.7$ eV between the first conduction band projected onto the $j_{\rm eff}=1/2$ state in the tetrahedral site and the second band projected onto the e_g state in the octahedral site [30]. We can exclude the presence of Cu metal, Cu^+ and Cu^{3+} ions, from the possible reason for the peak splitting because of the observed small splitting energy: for the latter cases, one expects to see much larger splitting in the order of a few electronvolts [43,44].

Moreover, the transition ratio at the L_3 and L_2 edges, or the branching ratio (BR), gives the expectation value $\langle \boldsymbol{l}\cdot\boldsymbol{s}\rangle$ of a hole state, and $\langle \boldsymbol{l}\cdot\boldsymbol{s}\rangle$ becomes zero for BR = 2 [28]. Therefore, in the octahedral site, the ratio of the spectral weight of peaks β and γ should follow the ratio of 2:1. The peak γ in Fig. 2(d) calculated using the half spectral weight of peak β is indeed comparable with the observed spectrum [30]. Finally, by subtracting the contribution of the octahedral site (peak β and γ) from the observed spectrum, we obtained the contribution solely from the tetrahedral site [30]. Using the resultant spectral weight at each edge, we evaluated BR in the tetrahedral site. It gives $\langle \boldsymbol{l}_{\rm eff}\cdot\boldsymbol{s}\rangle = 0.90(8)$, which is close to $\langle \boldsymbol{l}_{\rm eff}\cdot\boldsymbol{s}\rangle = 1$ of the $j_{\rm eff}=1/2$ state [28,45].

The SOE $J_{\rm eff}=1/2$ state of $CuAl_2O_4$ arises from the delicate balance among W, U, and λ [1,2]. Therefore, one can expect to induce various transitions of the SOE states according to the values of W, U, and λ by modifying the balance via adjusting a physical variable such as pressure [10–14]. Since the $J_{\rm eff}=1/2$ state of $CuAl_2O_4$ is in the exotic region of the phase diagram of U and λ, where large U and small λ make the strongly correlated spin-orbit regime [30], a novel phase transition distinct from those in the other $J_{\rm eff}=1/2$ states is expected to emerge by applying pressure.

To examine this possibility of a pressure-induced new phase, we carried out high-pressure XRD experiments to find the pressure-induced structural transition. Figure 3(a) shows that the Bragg peaks get split as pressure increases. The split Bragg peaks merge again and return to their initial phase as the pressure is released, ensuring that this pressure-induced transition is reversible. We also confirmed that the cubic lattice changes into a tetragonal lattice [30] with a space group of $I4_1/amd$ and a reduced lattice parameter $a_t=a_c/\sqrt{2}$, where a_c is the lattice parameter of the cubic phase.

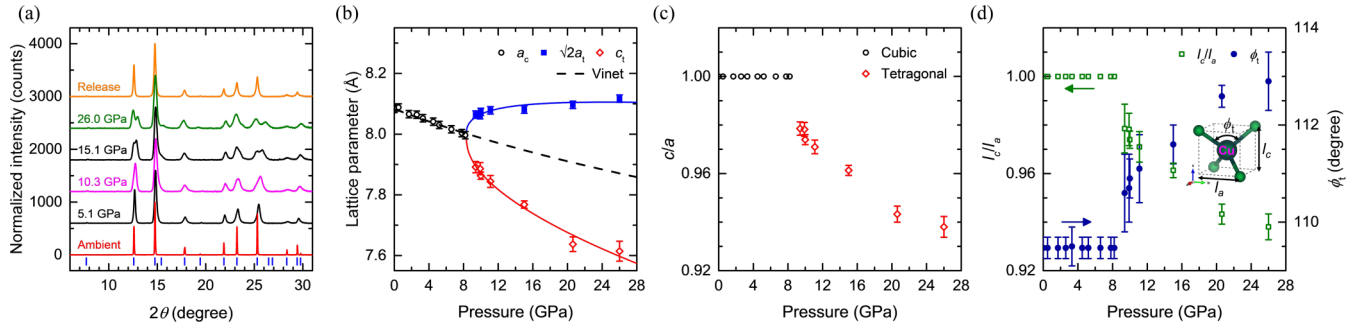

FIG. 3. (a) Pressure dependence of the x-ray diffraction (XRD) pattern. Peak splitting of Bragg peaks emerges under hydrostatic pressure, and the split merges back as the pressure is released. (b) Pressure dependence of the lattice parameters. The cubic phase transforms into a tetragonal phase above $P_c = 8(1)$ GPa. The lattice parameter of the cubic phase (a_c) was fitted to the Vinet equation of state (the dashed line), and those of the tetragonal phase (a_t and c_t) were fitted to a mean-field function proportional to $(P/P_c)^{\delta}$ (the solid line). (c) Pressure dependence of a ratio of lattice parameters c/a. Above P_c, it drops down from unity. (d) Pressure dependence of the O-Cu-O angle ϕ_t of the CuO_4 tetrahedron and the ratio of the height l_c to the base l_a of the tetrahedron.

According to our experimental data and subsequent analysis, a_c gets continuously reduced as pressure increases to the critical pressure $P_c \sim 8$ GPa [Fig. 3(b)]. The pressure dependence of a_c follows the typical Vinet equation of states [46] with a bulk modulus of $B_0 = 247(7)$ GPa and $dB_0/dP = 7$, comparable with those of other spinel compounds [47]. Above P_c, the structural transition emerges, and $\sqrt{2}a_t$ bifurcates from the lattice parameter along the c axis, c_t. Comparing with a_t, which is increasing slightly as the pressure increases [$\Delta(\sqrt{2}a_t) = 0.05(1)$ Å], notably c_t reduces dramatically [$\Delta(c_t) = -0.28(4)$ Å]. By fitting the pressure dependence of the lattice parameters of the tetragonal phase using a mean-field equation, we can evaluate the critical pressure of $P_c = 8(1)$ GPa.

Figure 3(c) shows the pressure dependence of a ratio of the lattice parameters c/a, where we plot $c_t/(\sqrt{2}a_t)$ for the tetragonal phase. Above P_c, the ratio drops down to 0.979(3) and keeps reducing while the pressure increases. The reduction of c/a comes mainly from the contraction of the CuO_4 tetrahedron. Depicted in Fig. 3(d), the O-Cu-O angle ϕ_t of the tetrahedron increases from 109.5° above P_c. Moreover, a ratio of the height l_c to the base l_a of the tetrahedron follows almost the same pressure dependence of global c/a.

To understand the mechanism underlying the pressure-induced structural phase transition in $CuAl_2O_4$, we performed DFT calculations. The ground state of $CuAl_2O_4$ at the ambient pressure is confirmed to be $J_{\text{eff}} = 1/2$ with the cubic lattice, and it remains robust even with a notable amount of site disorder $\eta = 0.5$ [30]. The total energy calculated from the $CuAl_2O_4$ lattice shows its global minimum locating at the point where the ratio of the lattice parameters c/a is unity [Fig. 4(a)]. However, as the pressure increases, the unit cell volume reduces, and the bond length of copper and oxygen ions becomes shorter. The lattice optimization calculations show the shift of the balance from the undistorted $J_{\text{eff}} = 1/2$ state to the state with $S = 1/2$ with Jahn-Teller distortion. As a result, the minimum of the total energy shifts suddenly toward $c/a < 1$ above the theoretical critical volume change of the unit cell $1 - (V_c/V_0) = 0.02$.

In Fig. 4(b), the mixing parameter and the ratio of lattice parameters reach a value of $\alpha' = 1/3$ and $c/a = 1$, respectively, below the volume change of 2%, which denotes the stabilization of the $J_{\text{eff}} = 1/2$ state with the cubic lattice. When the volume changes >2%, however, α' moves toward 1, and $c/a < 0.95$, suggesting that the disentangled $S = 1/2$ state with the compressed tetragonal lattice has been stabilized for the phase with a smaller volume.

The observed transition of the cubic lattice into the compressed tetragonal lattice corresponds to what we expected from the total energy calculation [Fig. 4(c)]. Therefore, our measurement supports the scenario where the ground state of $CuAl_2O_4$ changes from the SOE $J_{\text{eff}} = 1/2$ to the spin-only $S = 1/2$ state. The behavior of c/a, depending on the volume change, corresponds to the theoretical expectation within the error bar. There is a slight difference in the estimate of the critical value $1 - (V_c/V_0)$ between the experimental [2.9(6)%] and the theoretical (2%) values. It can be due to the limitation or error in determining U, which relates to the values of V_c and c/a in our method.

From the x-ray absorption and high-pressure XRD studies, we observed direct evidence of the $J_{\text{eff}} = 1/2$ state in $CuAl_2O_4$ at ambient pressure, leading to the cubic lattice. We also discovered the pressure-induced structural transition to the compressed tetragonal lattice, hosting the spin-only state. This observation corresponds well to what we expect from the $J_{\text{eff}} = 1/2$ state under the regime of strong correlation. The crystal structure of $CuAl_2O_4$, where the separation of tetrahedra and the large U cooperate in stabilizing the $J_{\text{eff}} = 1/2$ state of Cu^{2+}, also allows the pressure-dependent evolution of the $J_{\text{eff}} = 1/2$ state in an isolated "cage." Our finding of the strongly correlated SOE state in $CuAl_2O_4$ can thus provide insight into unexplored territory in the phase diagram of U and λ, where $3d$ transition metal ions stabilize the SOE state by competing with Jahn-Teller distortion. Another candidate with a similar effect may include Co^{2+} in an octahedral crystal field, which can host the $J_{\text{eff}} = 1/2$ state [48,49]. For instance, the CoO_6 octahedra of γ-$SiCo_2O_4$ [50,51] and $Ba_3CoSb_2O_9$ [52,53] are reported to have a D_{3d} point group symmetry instead of a C_{2h} driven by Jahn-Teller distortion. It is noted that another spinel compound $NiRh_2O_4$ [54], where Ni^{2+} is positioned at the tetrahedral site, yields magnetic entropy of $R\ln 6$ instead of

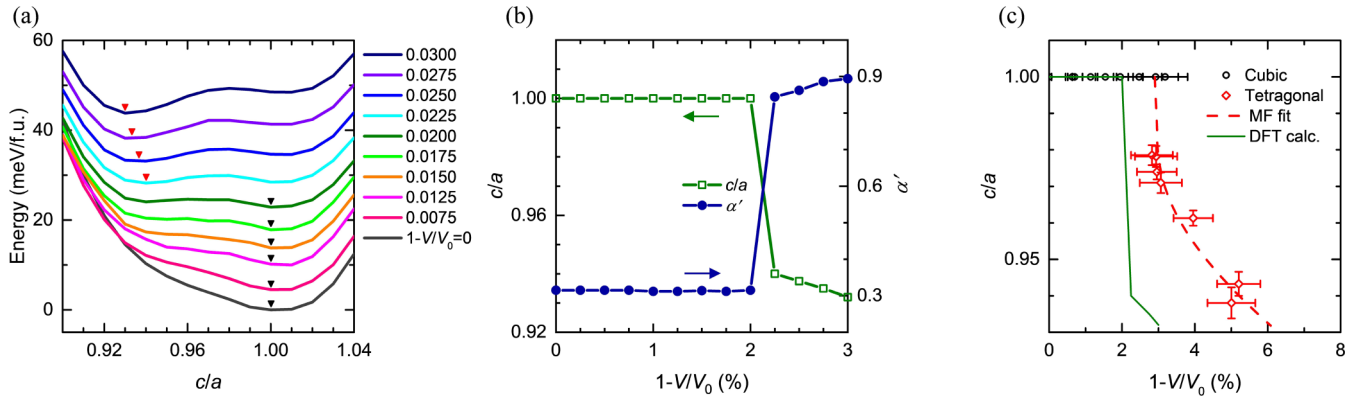

FIG. 4. (a) Calculated total energy depending on the change of the unit cell volume. The arrow denotes where the minima of the total energy locate. The global minimum shifts its position from $c/a = 1$ to $c/a < 1$ above the critical volume change of $1 - (V_c/V_0) = 0.02$. (b) Calculated volume change dependence of α' in Eq. (1) and c/a. The structural transition of the cubic to the tetragonal lattice at V_c accompanies a transition in the ground state from the $J_{\text{eff}} = 1/2$ to $S = 1/2$ states. (c) Comparison of c/a ratio depending on the volume change between the experimental data points (symbols) and two theoretical lines: one is that from the mean-field function (the dashed line) and another that from the DFT calculations in Fig. 3(b) (the solid line).

$R\ln 3$ of spin-only $S = 1$, which implies a ground state with entanglement.

It should be noted that the transition of the ground state from $J_{\text{eff}} = 1/2$ to $S = 1/2$ does not occur in other systems. For instance, in the Ruddlesden-Popper series of iridates $Sr_{n+1}Ir_nO_{3n+1}$ [10,11], the pressure broadens the bandwidth of t_{2g} states and eventually turns the ground state into a typical metal. In the case of the honeycomb-based Kitaev candidates α-Li_2IrO_3 [12], β-Li_2IrO_3 [13], and α-$RuCl_3$ [14], the pressure leads to dimerization, changing the Mott insulating $J_{\text{eff}} = 1/2$ phase to a gapped dimerized one.

Two mechanisms could, in principle, suppress the effect of SOC under pressure. One is the splitting of triply degenerate t_2 levels by extra distortions due to the Jahn-Teller effect. The other more substantial effect is the intersite electron hopping t and the corresponding formation of bands [55–57]. Since both effects become more critical with increasing electron hopping or the bandwidth, they will be enhanced by pressure, which could explain the novel transition from the SOE $J_{\text{eff}} = 1/2$ state at ambient pressure to the Jahn-Teller distorted $S = 1/2$ state at high pressure that we discovered in $CuAl_2O_4$.

In conclusion, we have successfully demonstrated that the $CuAl_2O_4$ has a $J_{\text{eff}} = 1/2$ state at ambient pressure, which undergoes a rare transition to an $S = 1/2$ state upon applying pressure. This pressure-driven transition between a $J_{\text{eff}} = 1/2$ state and an $S = 1/2$ state is well captured by the DFT calculations with the SOC fully employed. Our observation constitutes an observation of pressure-driven J_{eff}-to-S states with the intrinsically strong Coulomb interaction. Our paper offers an exciting opportunity to explore the spin-orbit entanglement at the regime of strong correlation.

We acknowledge helpful discussions with Wondong Kim, Roger Johnson, and Frank de Groot. This paper was supported by the Institute for Basic Science (IBS) in Korea [No. IBS-R009-G1 (H.C., T.K., C.K., J.G.P.) and No. IBS-R009-D1 (C.H.K.)] and the Leading Researchers Program of the National Research Foundation of Korea [NRF-2020R1A3B2079375 (T.K., C.K., J.G.P.), NRF-2019K1A3A7A09101574 (D.S.), and NRF-2020R1C1C1013642 (D.S.)]. H.C. acknowledges funding from the European Research Council (ERC) under the European Union's Horizon 2020 Research and Innovation Program Grant Agreement No. 788814. The work of D.I.Kh. was funded by the Deutsche Forschungsgemeinschaft (DFG, German Research Foundation) Project No. 277146847-CRC 1238. The synchrotron-based experiments were done in PAL and Photon Factory (Proposal No. 2017G644).

[1] W. Witczak-Krempa, G. Chen, Y. B. Kim, and L. Balents, Correlated quantum phenomena in the strong spin-orbit regime, Annu. Rev. Condens. Matter Phys. **5**, 57 (2014).

[2] B. J. Kim, H. Jin, S. J. Moon, J.-Y. Kim, B.-G. Park, C. S. Leem, J. Yu, T. W. Noh, C. Kim, S.-J. Oh, J.-H. Park, V. Durairaj, G. Cao, and E. Rotenberg, Novel $J_{\text{eff}} = 1/2$ Mott State Induced by Relativistic Spin-Orbit Coupling in Sr_2IrO_4, Phys. Rev. Lett. **101**, 076402 (2008).

[3] B. J. Kim, H. Ohsumi, T. Komesu, S. Sakai, T. Morita, H. Takagi, and T. Arima, Phase-sensitive observation of a spin-orbital Mott state in Sr_2IrO_4, Science **323**, 1329 (2009).

[4] D. I. Khomskii, *Transition Metal Compounds* (Cambridge Univ. Press, Cambridge, 2014).

[5] A. Georges, L. de Medici, and J. Mravlje, Strong correlations from Hund's coupling, Annu. Rev. Condens. Matter Phys. **4**, 137 (2013).

[6] G. Jackeli and G. Khaliullin, Mott Insulators in the Strong Spin-Orbit Coupling Limit: From Heisenberg to a Quantum Compass and Kitaev Models, Phys. Rev. Lett. **102**, 017205 (2009).

[7] K. Kitagawa, T. Takayama, Y. Matsumoto, A. Kato, R. Takano, Y. Kishimoto, S. Bette, R. Dinnebier, G. Jackeli, and H. Takagi, A spin–orbital-entangled quantum liquid on a honeycomb lattice, Nature **554**, 341 (2018).

[8] Y. Kasahara, T. Ohnishi, Y. Mizukami, O. Tanaka, Sixiao Ma, K. Sugii, N. Kurita, H. Tanaka, J. Nasu, Y. Motome, T. Shibauchi, and Y. Matsuda, Majorana quantization and half-integer thermal quantum Hall effect in a Kitaev spin liquid, Nature **559**, 227 (2018).

[9] S.-H. Do, S.-Y. Park, J. Yoshitake, J. Nasu, Y. Motome, Y. S. Kwon, D. T. Adroja, D. J. Voneshen, K. Kim, T.-H. Jang, J.-H. Park, K.-Y. Choi, and S. Ji, Majorana fermions in the Kitaev quantum spin system α-$RuCl_3$, Nat. Phys. **13**, 1079 (2017).

[10] C. Donnerer, Z. Feng, J. G. Vale, S. N. Andreev, I. V. Solovyev, E. C. Hunter, M. Hanfland, R. S. Perry, H. M. Rønnow, M. I. McMahon, V. V. Mazurenko, and D. F. McMorrow, Pressure dependence of the structure and electronic properties of $Sr_3Ir_2O_7$, Phys. Rev. B **93**, 174118 (2016).

[11] D. Haskel, G. Fabbris, Mikhail Zhernenkov, P. P. Kong, C. Q. Jin, G. Cao, and M. van Veenendaal, Pressure Tuning of the Spin-Orbit Coupled Ground state in Sr_2IrO_4, Phys. Rev. Lett. **109**, 027204 (2012).

[12] V. Hermann, M. Altmeyer, J. Ebad-Allah, F. Freund, A. Jesche, A. A. Tsirlin, M. Hanfland, P. Gegenwart, I. I. Mazin, D. I. Khomskii, R. Valentí, and C. A. Kuntscher, Competition between spin-orbit coupling, magnetism, and dimerization in the honeycomb iridates: α-Li_2IrO_3 under pressure, Phys. Rev. B **97**, 020104(R) (2018).

[13] T. Takayama, A. Krajewska, A. S. Gibbs, A. N. Yaresko, H. Ishii, H. Yamaoka, K. Ishii, N. Hiraoka, N. P. Funnell, C. L. Bull, and H. Takagi, Pressure-induced collapse of the spin-orbital Mott state in the hyperhoneycomb iridate β-Li_2IrO_3, Phys. Rev. B **99**, 125127 (2019).

[14] G. Bastien, G. Garbarino, R. Yadav, F. J. Martinez-Casado, R. Beltrán Rodríguez, Q. Stahl, M. Kusch, S. P. Limandri, R. Ray, P. Lampen-Kelley, D. G. Mandrus, S. E. Nagler, M. Roslova, A. Isaeva, T. Doert, L. Hozoi, A. U. B. Wolter, B. Büchner, J. Geck, and J. van den Brink, Pressure-induced dimerization and valence bond crystal formation in the Kitaev-Heisenberg magnet α-$RuCl_3$, Phys. Rev. B **97**, 241108(R) (2018).

[15] K. W. Plumb, J. P. Clancy, L. J. Sandilands, V. Vijay Shankar, Y. F. Hu, K. S. Burch, H.-Y. Kee, and Y.-J. Kim, α-$RuCl_3$: A spin-orbit assisted Mott insulator on a honeycomb lattice, Phys. Rev. B **90**, 041112(R) (2014).

[16] A. Banerjee, C. A. Bridges, J.-Q. Yan, A. A. Aczel, L. Li, M. B. Stone, G. E. Granroth, M. D. Lumsden, Y. Yiu, J. Knolle, S. Bhattacharjee, D. L. Kovrizhin, R. Moessner, D. A. Tennant, D. G. Mandrus, and S. E. Nagler, Proximate Kitaev quantum spin liquid behaviour in a honeycomb magnet, Nat. Mater. **15**, 733 (2016).

[17] G. Cao and P. Schlottmann, The challenge of spin–orbit-tuned ground states in iridates: A key issues review, Rep. Prog. Phys. **81**, 042502 (2018).

[18] R. Nirmala, K.-H. Jang, H. Sim, H. Cho, J. Lee, N.-G. Yang, S. Lee, R. M. Ibberson, K. Kakurai, M. Matsuda, S.-W. Cheong, V. V. Gapontsev, S. V. Streltsov, and J.-G. Park, Spin glass behavior in frustrated quantum spin system $CuAl_2O_4$ with a possible orbital liquid state, J. Phys.: Condens. Matter **29**, 13LT01 (2017).

[19] H. Cho, R. Nirmala, J. Jeong, P. J. Baker, H. Takeda, N. Mera, S. J. Blundell, M. Takigawa, D. T. Adroja, and J.-G. Park, Dynamic spin fluctuations in the frustrated A-site spinel $CuAl_2O_4$, Phys. Rev. B **102**, 014439 (2020).

[20] C. H. Kim, S. Baidya, H. Cho, V. V. Gapontsev, S. V. Streltsov, D. I. Khomskii, J.-G. Park, A. Go, and H. Jin, Theoretical evidence of spin-orbital-entangled $J_{\text{eff}} = 1/2$ state in the $3d$ transition metal oxide $CuAl_2O_4$, Phys. Rev. B **100**, 161104(R) (2019).

[21] S. A. Nikolaev, I. V. Solovyev, A. N. Ignatenko, V. Y. Irkhin, and S. V. Streltsov, Realization of the anisotropic compass model on the diamond lattice of Cu^{2+} in $CuAl_2O_4$, Phys. Rev. B **98**, 201106(R) (2018).

[22] T. Yamamoto, Assignment of pre-edge peaks in K-edge x-ray absorption spectra of $3d$ transition metal compounds: Electric dipole or quadrupole, X-Ray Spectrom. **37**, 572 (2008).

[23] S. E. Shadle, J. E. Penner-Hahn, H. J. Schugar, B. Hedman, K. O. Hodgson, and E. I. Solomon, X-ray absorption spectroscopic studies of the blue copper site: Metal and ligand K-edge studies to probe the origin of the EPR hyperfine splitting in plastocyanin, J. Am. Chem. Soc. **115**, 767 (1993).

[24] T. Tangcharoen, W. Klysubun, and C. Kongmark, Synchrotron x-ray absorption spectroscopy and cation distribution studies of $NiAl_2O_4$, $CuAl_2O_4$, and $ZnAl_2O_4$ nanoparticles synthesized by sol-gel auto combustion method, J. Mol. Struct. **1182**, 219 (2019).

[25] J. A. van Bokhoven and C. Lamberti, *X-Ray Absorption and X-Ray Emission Spectroscopy: Theory and Applications* (Wiley, New York, 2016).

[26] A. L. Ankudinov, B. Ravel, J. J. Rehr, and S. D. Conradson, Real-space multiple-scattering calculation and interpretation of x-ray-absorption near-edge structure, Phys. Rev. B **58**, 7565 (1998).

[27] J. P. Clancy, N. Chen, C. Y. Kim, W. F. Chen, K. W. Plumb, B. C. Jeon, T. W. Noh, and Y.-J. Kim, Spin-orbit coupling in iridium-based $5d$ compounds probed by x-ray absorption spectroscopy, Phys. Rev. B **86**, 195131 (2012).

[28] B. T. Thole and G. van der Laan, Linear relation between x-ray absorption branching ratio and valence-band spin-orbit expectation value, Phys. Rev. A **38**, 1943 (1988).

[29] D.-Y. Cho, J. Park, J. Yu, and J.-G. Park, X-ray absorption spectroscopy studies of spin-orbit coupling in $5d$ transition metal oxides, J. Phys.: Condens. Matter **24**, 055503 (2012).

[30] See Supplemental Material at http://link.aps.org/supplemental/10.1103/PhysRevB.103.L081101 for further details of the experimental and theoretical methods and supporting data. The Supplemental Material includes references [31–42].

[31] B. Ravel and M. Newville, Athena, Artemis, Hephaestus: data analysis for x-ray absorption spectroscopy using IFEFFIT, J. Synchrotron Rad. **12**, 537 (2005).

[32] R. Sarangi, S. D. George, D. J. Rudd, R. K. Szilagyi, X. Ribas, C. Rovira, M. Almeida, K. O. Hodgson, B. Hedman, and E. I. Solomon, Sulfur K-edge x-ray absorption spectroscopy as a probe of ligand-metal bond covalency: Metal vs ligand oxidation in copper and nickel dithiolene complexes, J. Am. Chem. Soc. **129**, 2316 (2007), and its supporting information.

[33] E. Antonides, E. C. Janse, and G. A. Sawatzky, LMM auger spectra of Cu, Zn, Ga, and Ge. I. Transition probabilities, term splittings, and effective Coulomb interaction, Phys. Rev. B **15**, 1669 (1977).

[34] M. I. Aroyo, J. M. Perez-Mato, C. Capillas, E. Kroumova, S. Ivantchev, G. Madariaga, A. Kirov, and H. Wondratschek, Bilbao crystallographic server: I. databases and crystallographic computing programs, Z. Kristallogr. **221**, 15 (2006); M. I. Aroyo, A. Kirov, C. Capillas, J. M. Perez-Mato, and H. Wondratschek, Bilbao crystallographic server. II. Representations of crystallographic point groups and space groups, Acta Cryst. **A62**, 115 (2006).

[35] P. W. Stephens, Phenomenological model of anisotropic peak broadening in powder diffraction, J. Appl. Cryst. **32**, 281 (1999).

[36] J. Rodriguez-Carvajal, Recent advances in magnetic structure determination by neutron powder diffraction, Physica B **192**, 55 (1993).

[37] A. V. Zakrzewski, S. Gangopadhyay, G. J. MacDougall, A. A. Aczel, S. Calder, and T. J. Williams, Evolution of magnetic and orbital properties in the magnetically diluted A-site spinel $Cu_{1-x}Zn_xRh_2O_4$ Phys. Rev. B **97**, 214411 (2018).

[38] A. L. Bail, Whole powder pattern decomposition methods and applications: a retrospection, Powder Diffr. **20**, 316 (2005).

[39] H. M. Rietveld, A profile refinement method for nuclear and magnetic structures, J. Appl. Cryst. **2**, 65 (1969).

[40] J. P. Perdew, A. Ruzsinszky, G. I. Csonka, O. A. Vydrov, G. E. Scuseria, L. A. Constantin, X. Zhou, and K. Burke, Restoring the Density-Gradient Expansion for Exchange in Solids and Surfaces, Phys. Rev. Lett. **100**, 136406 (2008).

[41] http://elk.sourceforge.net.

[42] S. L. Dudarev, G. A. Botton, S. Y. Savrasov, C. J. Humphreys, and A. P. Sutton, Electron-energy-loss spectra and the structural stability of nickel oxide: an LSDA+U study, Phys. Rev. B **57**, 1505 (1998).

[43] P. Jiang, D. Prendergast, F. Borondics, S. Porsgaard, L. Giovanetti, E. Pach, J. Newberg, H. Bluhm, F. Besenbacher, and M. Salmeron, Experimental and theoretical investigation of the electronic structure of Cu_2O and CuO thin films on Cu(110) using x-ray photoelectron and absorption spectroscopy, J. Chem. Phys. **138**, 024704 (2013).

[44] R. Sarangi, N. Aboelella, K. Fujisawa, W. B. Tolman, B. Hedman, K. O. Hodgson, and E. I. Solomon, X-ray absorption edge spectroscopy and computational studies on $LCuO_2$ species: Superoxide-CuII versus peroxide-CuIII bonding, J. Am. Chem. Soc. **128**, 8286 (2006).

[45] J.-H. Sim, H. Yoon, S. H. Park, and M. J. Han, Calculating branching ratio and spin-orbit coupling from first principles: A formalism and its application to iridates, Phys. Rev. B **94**, 115149 (2016).

[46] P. Vinet, J. R. Smith, J. Ferrante, and J. H. Rose, Temperature effects on the universal equation of state of solids, Phys. Rev. B **35**, 1945 (1987).

[47] D. Errandonea, AB_2O_4 compounds at high pressures, in *Pressure-Induced Phase Transitions in AB_2X_4 Chalcogenide Compounds*, edited by F. J. Manjon, I. Tiginyanu, and V. Ursaki (Springer, Berlin, 2014), Chap. 2.

[48] H. Liu and G. Khaliullin, Pseudospin exchange interactions in d^7 cobalt compounds: Possible realization of the Kitaev model, Phys. Rev. B **97**, 014407 (2018).

[49] H. Liu, J. Chaloupka, and G. Khaliullin, Kitaev Spin Liquid in 3*d* Transition Metal Compounds, Phys. Rev. Lett. **125**, 047201 (2020).

[50] F. Marumo, M. Isobe, and S. Akimoto, Electron-density distributions in crystals of γ-Fe_2SiO_4 and γ-Co_2SiO_4, Acta Cryst. B**33**, 713 (1977).

[51] W. Zhang, S. Okubo, H. Ohta, T. Saito, and M. Takano, High-frequency ESR measurements of the Co spinel compound $SiCo_2O_4$, J. Phys.: Condens. Matter **19**, 145264 (2007).

[52] Y. Doi, Y. Hinatsu, and K. Ohoyama, Structural and magnetic properties of pseudo-two-dimensional triangular antiferromagnets $Ba_3MSb_2O_9$ (M = Mn, Co, and Ni), J. Phys.: Condens. Matter **16**, 8923 (2004).

[53] Y. Shirata, H. Tanaka, A. Matsuo, and K. Kindo, Experimental Realization of a Spin-1/2 Triangular-Lattice Heisenberg Antiferromagnet, Phys. Rev. Lett. **108**, 057205 (2012).

[54] J. R. Chamorro, L. Ge, J. Flynn, M. A. Subramanian, M. Mourigal, and T. M. McQueen, Frustrated spin one on a diamond lattice in $NiRh_2O_4$, Phys. Rev. Mater. **2**, 034404 (2018).

[55] S. V. Streltsov and D. I. Khomskii, Covalent bonds against magnetism in transition metal compounds, Proc. Natl. Acad. Sci. USA **113**, 10491 (2016).

[56] M. Ye, H.-S. Kim, J.-W. Kim, C.-J. Won, K. Haule, D. Vanderbilt, S.-W. Cheong, and G. Blumberg, Covalency-driven collapse of strong spin-orbit coupling in face-sharing iridium octahedra, Phys. Rev. B **98**, 201105(R) (2018).

[57] D. I. Khomskii and S. V. Streltsov, Orbital effects in solids: Basics and novel development, Chem. Rev. 2020.